RESEARCH ARTICLE

Anti-CSC Effects in Human Esophageal Squamous Cell Carcinomas and Eca109/9706 Cells Induced by Nanoliposomal Quercetin Alone or Combined with CD 133 Antiserum

Nai-Gang Zheng[1,2]*, Sai-Jun Mo[1,2], Jin-Ping Li[1], Jing-Lan Wu[1]

Abstract

CD133 was recently reported to be a cancer stem cell and prognostic marker. Quercetin is considered as a potential chemopreventive agent due to its involvement in suppression of oxidative stress, proliferation and metastasis. In this study, the expression of CD133/CD44 in esophageal carcinomas and Eca109/9706 cells was explored. In immunoflurorescence the locations of CD133$^+$ and multidrug resistance 1 (MDR 1)$^+$ in the same E-cancer cells were coincident, mainly in cytomembranes. In esophageal squamous cell carcinomas detected by double/single immunocytochemistry, small CD133$^+$ cells were located in the basal layer of stratified squamous epithelium, determined as CSLC (cancer stem like cells); CD44$^+$ surrounding the cells appeared in diffuse pattern, and the larger CD44$^+$ (hi) cells were mainly located in the prickle cell layer of the epithelium, as progenitor cells. In E-cancer cells exposed to nanoliposomal quercetin (nLQ with cytomembrane permeability), down-regulation of NF-κBp65, histone deacetylase 1 (HDAC1) and cyclin D1 and up-regulation of caspase-3 were shown by immunoblotting, and attenuated HDAC1 with nuclear translocation and promoted E-cadherin expression were demonstrated by immunocytochemistry. In particular, enhanced E-cadherin expression reflected the reversed epithelial mesenchymal transition (EMT) capacity of nLQ, acting as cancer attenuator/preventive agent. nLQ acting as an HDAC inhibitor induced apoptotic cells detected by TUNEL assay mediated via HDAC-NF-κB signaling. Apoptotic effects of liposomal quercetin (LQ, with cytomembrane-philia) combined with CD133 antiserum were also detected by CD133 immunocytochemistry combined with TUNEL assay. The combination could induce greater apoptotic effects than nLQ induced alone, suggesting a novel anti-CSC treatment strategy.

Keywords: CSC marker - nanoliposomal/liposomal quercetin - human esophageal SCC - treatment strategy

Asian Pac J Cancer Prev, **15 (20)**, 8679-8684

Introduction

The cancer stem cell, CSC, also referred as cancer initiating cell, CIC, plays pivotal role in carcinogenesis, progression and metastasis. CSC/CIC possesses higher resistance to chemotherapy/radiotherapy and apoptosis than cancer cells, which can result in ineffective treatment and cancer relapse after treatment (Cetin and Topcul, 2012). Studies of CSC key markers principally aimed at selective elimination or establishment of therapeutic/preventive target have become international hot spot in cancer research. CD133 is a universal marker used to identify and isolate normal stem cells (SC) or CSC from various organs or tumors (Tabu et al., 2013; Puglisi et al., 2009). A small subpopulation with stem cell properties, responsible for initiation of new tumor formation was selected by CD44$^+$/CD24(-/low) marker in breast cancer (Carcia Bueno, 2008). A subpopulation of colon cells with CD44(hi$^+$) has been identified to be highly tumorigenic as stem-like cells (Chu et al., 2009). CD44 is cell surface molecule proposed to identify cancer stem/progenitor cells in prostate cancer (Simon et al., 2009). However, it has been found in advanced study that prominin-1 CD133 also expressed in the prostate cancer, pancreatic cancer, breast cancer and colon cancer either as additional CSC marker or as prognostic marker (Aomatsu et al., 2012; Wang et al., 2012; Hori, 2013; Pellacani et al., 2013).

After birth definite numbers of stem cells (SC) reside at the basal layer of stratified squamous epithelium or the basal portion of intestinal crypts, suggesting that these areas would greatly contribute to detection of stem cell marker (Pincelli and Marconi, 2010). Overexpression of the tissue factor accompanies cellular aggressive features, such as CD133 marker, epithelial-to-mesenchymal transition (EMT) and expression of angiogenic and prometastatic phenotype to play an important role in formation of the vascular niche for CSC (Pincelli et al.,2010). We think that the anti-CSC marker effect could contribute to inhibiting cancer aggressive and prometastatic features.

In our previous work we isolated the stem/progenitor

[1]*Molecular Cell Biology Research Center,* [2]*Department of Basic Science of Oncology, Medical College of Zhengzhou University, Zhengzhou, China *For correspondence: zhengng@zzu.edu.cn*

like cells with $p63^+/k19^+$ marker by filter screening combined with immunoabsorbant assay from the normal skin biopsy, and the cultured colony spheres could reform a new confluent epidermis above the fibroblast feeder underground. In addition, we found that the isolated keratinocytes from the skin epidermis were different in sizes (6μ/7μ-30μ), the small cells with the stem marker(hi) reside on the basal membrane, and the middle sized cells with certain marker$^+$ located in the prickle cell layer of the epithelium, but no marker was found in the largest cells located at superficial layer of the epithelium (Zheng, et al., 2008).

Based on down-regulated ROS stress and cell cycle progression in NIH3T3 cells, E-cancer cells, etc., and facilitating differentiation and apoptosis induced by quercetin in our previous experiments (Gong et al., 2009; Zhang et al., 2007), we found that the natural flavonoid quercetin could persist cell ROS in certain normal level, not only to down–regulate ROS to cells with higher ROS level, but also to up-regulate ROS to cells with lower ROS level. There are some anti-CSC studies in breast, leukemia and glioma tumors induced by green tea polyphenol, curcumin, resveratrol and other polyphenols (Chen et al., 2008; Charpentier et al., 2014). However, the information about quercetin anti-CSC effects in human esophageal stratified squamoous epiththelial cancer has been limited. In this study we designed to first detect CSC marker location in Eca109/9706 cells/human esophageal squamous cell carcinoma (ESCC) by immunofluorescene/ immunoenzyme technique. Then we first determined the water-soluble nanoliposomal quercetin (nLQ, with cytomembrane permeability) effect on E-cancer cells by immunoblotting, immunocytochemistry and TUNEL assay. Finally we examined apoptosis induced by water-soluble liposomal quercetin (LQ, with cytomembranephilia) combined with CD133 antiserum in E-cancer cells by CD133 immunocytochemistry andTUNEL assay.

Materials and Methods

Preparation of liposomal/nanoliposomal quercetin

Since quercetin is hardly dissoluble into water, we prepared liposomal/ nanoliposomal quercetin as follows. The quercetin (Sigma, USA), cholesterol, lecithecin, encephalin and polyethyleneglycol 4000 were mixed in ratio of 6:4:9:5:1, dissolved completely in chloroform/methanol (3:1), The dissolvent was processed by revolutionary evaporation under vacuum for 4-8h, hydrolyzed in PBS, repeated frozen-thawing several times, and finally passed through 220μm filter to obtain liposomal quercetin (LQ), 4.8mg/ml in PBS as stocking solution. The nanoliposomal quercetin (nLQ) was prepared by Sonics repeatedly until passing through a filter membrane with 80 nm pore size (Sigma, USA).

Cultivation of Eca109/9706 cells

The Eca109/9706 cell line preserved in our laboratory were recovered from liquid nitrogen and cultivated in DMEM medium (Sigma, USA) supplemented with 10% FBS (TBD, China) in humidified incubator (Sanyo, Japan) with 5% CO_2 at 36.5ºC

Double immunofluorescence staining

The intact E-cancer (Eca109/9706) cells on slides were fixed with 4% paraformaldehye for 10min, followed by heat-retrieval in microwave oven for 5min. Each slide was incubated simultaneously with double primary monoclonal antibodies, including CD133 against rabbit (BIOS, China) and MDR1 against mouse (SC, USA) in dilution 1:100 at 4ºC overnight. Next morning each slide was washed with PBS and incubated simultaneously with secondary antibodies, including sheep anti-rabbit IgG-TRITC (Jackson, USA) and sheep anti-mouse IgG-FITC (Jackson, USA) in 1:50 dilution. The primary antibody replaced by PBS was performed as negative control. Each slide was respectively activated with 518nm emissive wave length and with 616nm emissive wave length to reveal different colored fluorescence under fluorescent microscope and photographed.

Double/single immunocytochemistry

The E-cancer cell slides and the deparaffinized ESCC slides (from 10 patients' surgically resected ESCC tissues embedded in one paraffin block) were fixed with 4% paraformaldehyde and treated with heat–retrieval for 5 min. The slides were pretreated with H_2O_2/levomizol respectively to remove the endogenous peroxidase/ alkaline phosphatase(ALP). The slide was incubated with double primary CD133 and CD44 (anti-mouse, Zymed USA) antisera simultaneously in 1:100 dilution at 4ºC overnight. Then, the slides were washed with PBS and incubated firstly with secondary antibody of anti-mouse IgG-HRP in 1:100 dilution at 37 ºC for 30min, followed by incubation in DAB substrate to develop brownish color. Subsequently the slide re-incubated with secondary antibody of anti-rabbit IgG-ALP in 1:100 diluted for 30 min, and bluish-violet color developed by NBT-BCIP (Promega, USA) substrate. The primary antibody replaced by PBS was performed as the negative control. The slides were observed under microscope and photographed.

Immunoblotting of E-cancer cells induced by nLQ

The total protein was extracted from each group of E-cancer cells, including nLQ (nanoliposomal quercetin) and control groups, by using Cell Lysis Reagent (CelLytic™, Sigma, USA) and the protein concentration was measured with Bradford method. The SDS-PAGE gel was electro-transferred onto the pre-treated nitrocellulose membrane (NCM, Protran, USA). The primary antibodies, including anti-HDAC1 (polyclonal, Santa Cruz, USA), anti-NF-ϰBp65 (monoclonal, Santa Cruz, USA), anti-Cyclin D1 (monoclonal, Zymed, USA), anti-Caspase-3 (polyclonal, Zymed, USA) and anti-β-actin (polyclonal, ZSGB, China) were incubated with corresponding NCM on a vibrator under room temperature for 2.5h. The TTBS buffer (0.15mol/L NaCl and 0.05% Tween 20 added into 0.1mol/L Tris-Cl buffer, pH 7.5) was used as blocking or washing solution. The goat or mouse IgG-HRP (monoclonal ZSGB, China) was used as the secondary antibody to incubate the NCM on a vibrator under room temperature for 1.5h, finally the brownish color developed on the NCM under DAB substrate for 20min. The anti-β-actin was added into each lane as loading control. The grey

scaled means (GSM) for target bands were determined by an Image-Scanner (ShanFu, China).

Immunocytochemistry of HDAC1/ E-cadherin in E-cancer cells induced by nLQ

The cell specimens from nLQ (nanoliposomal quercetin) and control groups were fixed with 4% paraformaldehyde, followed by treatment with 0.3% Triton-X100/PBS and subsequently blocking with normal serum. The anti-HDAC1 serum or anti-E-cadherin (monoclonal, Zymed, USA) was used as primary antibody, the SP kit (ZhongShan, China) was used as secondary and tertiary anti-sera. Finally the brownish signals developed under DAB substrate. The primary antibody replaced by PBS was performed as the negative control. The GSM of immunoreactivity (IR) signals were scanned by an Image-Scanner (ShanFu, China).

E-cancer cells apoptosis induced by nLQ detected by TUNEL assay

The cultured E-cancer cells were divided into 2 groups: nLQ: cultured with 40μmol nLQ for 48h; C (control): cultured without nLQ for 48h. After the cell slides were fixed by 4% paraformaldehyde, the TUNEL assay was carried out as follows. The slides were digested with 5μg/ml proteinase K (Promega, USA), 37ºC for 10 min, washing and re-fixed with paraformaldehyde for 5min. Each slide was incubated with 15μl TdT buffer containing 0.5μl TdT enzyme (TdT, terminal deoxyribonucleotide transferase, Promega, USA), 0.5μl Biotin-16-dUTP (Rouche, Germany) at 4ºC overnight; followed by incubation with 1:800 diluted streptavidin-ALP (Promega, USA) about 40 min under 37°C, washing with Tris-Cl buffer pH7.5 and re-washing with Tris-Cl buffer pH9.5 several times. Finally bluish-violet apoptotic signals were demonstrated by NBT-BCIP substrate on the slide. The negative control substituted TdT buffer for TdT enzyme.

E-cancer cells apoptosis induced by LQ and CD133 antiserum detected by CD133 immunocytochemistry combined with TUNEL assay

Since the CD133 marker was mainly located at the cytomambrane, the CD133 antiserum combined with liposomal quercetin (LQ with cytomembrane-Philia) would contribute to inducing apoptosis. The cultured Eca109/9706 cells were divided into 3 groups: LQ+CD133 antiserum: co-cultured with 1.6 μl 40μmol LQ combined with 12μl CD133 antibody (the ratio of liposome and protein is about 2:3 in component, similar to that in normal cytomembrane) for 48h, LQ alone: only cultured with 40μmol LQ for 48h and control: treated with neither LQ nor CD133 antiserum for 48h. The paraformaldehyde fixed cell slides were first stained by immunocytochemistry with SP kit (ZSGB, China) to demonstrate yellow-brownish signals of CD133 marker under DAB substrate. Subsequently TUNEL assay was carried out on the cell slides as mentioned above.

Statistical analysis

Statistical analyses were performed by use of SPSS 17.0 statistical package. The data shown as ($\bar{\chi}\pm$s) represented at least three independent experiments: In each slide of TUNEL assay 200 cells were enumerated as the apoptotic rate. The difference was analyzed with one way ANOV: $p<0.05$ was considered as significant level.

Results

Double immunofluorescence in E-cancer cells

In E-cancer cells stained by double immunofluorescence with anti-CD133 and anti-MDR1, the CD133$^+$ displayed red-colored fluorescene, the MDR1$^+$ displayed green-colored fluorescene. Both positive fluorescene signals were mainly localized at the same intact cells cytomembrane with coincident intensity and location (Figure 1Aa, Figure 1Ba).

Immunoenzyme of CD133/CD44 in E-cancer cells

About 75% E-cancer cells showed CD133$^+$/CD44$^+$ with different intensity. In E-cancer cell slides CD133$^+$ appeared as bluish-violet fine granules mainly located at the intact cell cytomembrane in different sized cells (Figure 1Ca). The distinct CD44$^+$ brownish–yellow granules surrounded the E-cancer cells in diffuse pattern (Figure 1Ab).

Double/single immunohistocytochemistry of CD133/ CD44 in ESCC

A small subpopulation of 8% Eca109/ 6% 9706 cells were small sized (≈red blood cell-small lymphocyte). The small CD44$^+$ brownish-yellow cells only reside at the basal layer of stratified squamous epithelium, the larger cells with CD44$^+$ (hi) were mainly located in the prickle cell layer of the epithelium (Figure 1 Bb). The small distinct brownish-violet CD133$^+$CD44$^+$ cells were located at the basal layer of the stratified squamous epithelium (Figure 1Cb) stained by CD133+CD44 double immunoenzyme staining. In ESCC connective tissue the small CD133$^+$ cells with bluish-violet granules were located at the cancer pear periphery (corresponding to the epithelial basal layer) or scattered in cancer focus.

Immunoblotting of HDAC1, NF-$\varkappa$Bp65, Cyclin D1, Caspase-3 in E-cancer cells induced by nLQ

When compared with control (C) group, nLQ could induce HDAC1, NF-$\varkappa$Bp65 and Cyclin D1 down-regulated, Caspase-3 up-regulated (Table 1, Figure 2Aa, 2Ab).

Immunocytochemistry of HDAC1/E-cadherin in E-cancer cells induced by nLQ

The intense HDAC1-immunoreactivity (IR) in dark

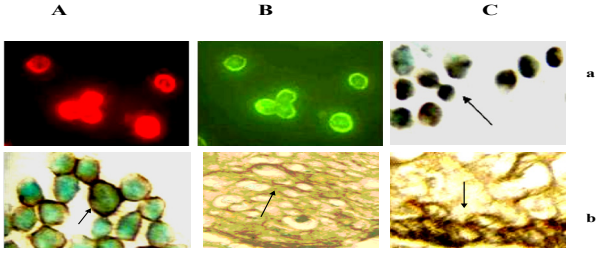

Figure 1. CSC markers in E-cancer cells/ESCC

Table 1. GSM ($\bar{\chi}$±s) for the ratio of β-Actin and Respective Immunoblottings

Index/group	nLQ	Control
HDAC1	0.591±0.006*,	0.702±0.003
NF-ϰBp65	0.787±0.004*	0.901±0.005
Cyclin D1	0.299±0.002*	0.665±0.005
Caspase- 3	0.620±0.001*	0.480±0.005

*C; P<0.05

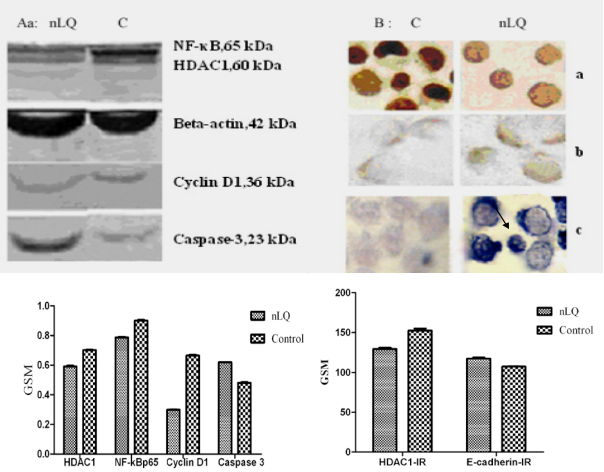

Figure 2. nLQ Effect on E-cancer Cells. 2Aa:immunoblotting, 2Ba:HDAC1-IR, 2Bb-Cadherin-IR, 2Bc:apoptosis, 2Ab:Diagram of Immnunoblotting in nLQ vs C, 2Bab:Diagram of HDAC1-IR, Cadherin-IR in nLQ vs C

brownish granules was mainly located in the nuclei (nuclear pattern) in the control group, while the nLQ group appeared cytoplasm/mixed pattern (translocated from nuclear pattern in the control) with attenuated HDAC1-IR (Table 2, Figure 2Ba). The E-cadherin-IR located at the intact cells surface in nLQ group was stronger than that in the control group (Table 2, Figure 2Bb).

E-cancer cells apoptosis induced by nLQ detected by TUNEL assay

In the nLQ group the apoptotic bluish violet signals in semi-lunar shape were mainly located at the periphery of the apoptotic cells which were different in sizes, but with no CSC marker demonstrated. The apoptotic body attached to the apoptotic cells also could be found. The apoptotic signals could be scarcely found in the control (C) group (Figure 2Bc). The difference in apoptotic rates between two groups of Eca9706 cells (nLQ group: 42.5±0.5%; C group: 4.5±0.5%,) was significant, p<0.05.

E-cancer cells apoptosis induced by LQ+CD133 antiserum detected by CD133 immunocytochemistry combined with TUNEL assay

In the group of LQ+CD133 antiserum the violet-bluish apoptotic signals in semi-lunar shape were mainly located at periphery of CD133$^+$ apoptotic cells with different sizes, after firstly stained in yellow-brownish color by CD133 immunocytochemistry followed by violet apoptoic signals through TUNEL assay. The apoptotic body attached to the apoptotic cells also could be seen. Among apoptotic cells there were two small apoptotic cells with mixed brownish-violet signals (Figure 3A). In the LQ group only induced

Table 2. GSM ($\bar{\chi}$±s) of HDAC1-IR/E-Cadherin-IR in E-Cancer Cells Induced by nLQ Compared with C Group

Index/Group	nLQ	Control
HDAC1-IR	129.32±1.65*	152.61±2.59
E-cadherin-IR	117.36 ±1.22*	107.24±0.24

*C; P<0.05

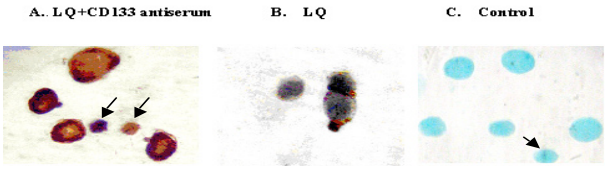

Figure 3. Apoptotic Effect Induced by LQ Combined CD133 Antiserum on Eca109 Cells

by LQ alone, the bluish-violet apoptotic signals as fine granules were mainly located in the cells with no distinct yellow-brownish colored CD133$^+$ marker demonstrated. The apoptotic body attached the apoptotic cells also could be found (Figure 3B). However, the intracellular apoptotic signals in Figure 3A and Figure 3B were not so clear as that induced by nLQ in the Figure 2Bc. In the control group, the violet apoptotic signal could be scarcely found (Figure 3C). The difference in apoptotic rates among three groups was significant. The apoptotic rates in Eca109 cells were group A: 49.5±0.5%, group B: 42.5±0.5% and group C: 5.0±0.5%, p<0.05; in Eca9706 cells, group A: 47.5±0.5%, group B: 40.5±0.5% and group C: 5.0±0.5%, p<0.05. In Eca109/9706 cells group A >group B was significant, p<0.05, while there was no significant difference in apoptotic rates between Eca109 cell group and Eca9706 cell group, p>0.05.

Discussion

Immunocytochemistry, including immunoenzyme and immunofluorescence is commonly used for detection of CSC/CSLC marker. Chen YC et al isolated both CD133$^+$ and CD133$^-$ cells from non small cell lung cancer and lung cancer cell lines, and found that CD133$^+$ cells displayed higher Oct-4 expression with significant resistance to chemotherapeutic agents (Hu et al., 2012). Bertrand J et al collected two major subpopulations from a human glioblastoma cell line, sedimentation by cell sorting: a most differentiated large cells sensitive to Fas-induced apoptosis and another characterized by small cells expressing CD133 marker and more resistant to Fas-induced apoptosis (Bertrand et al., 2009). In the present study CD133$^+$/MDR$^+$ cells were detected by double immunofluorescence with coincident intensity, suggesting that the CD133$^+$ cells may also possess resistance to multidrug.

Moreover, Bertrand J et al identified CSC/CSLC with emphasis on cell sizes, he found that the small cells forming aggregates and expressing CD133 were CSC in glioma (Bertrand et al., 2009). CD133 may be expressed in small sized quiescent CSC as well as in large sized differentiated cells, since CD133 is also expressed in differentiated cells (Tabu, et al., 2013). In the present

experiment the bluish-violet CD133+ cells in different sizes could constitutively expressed the distinct marker located mainly at cytomembrane in E-cancer cells. The small violet CD133+ cells were located at the basal layer of stratified squamous epithelium in ESCC, suggesting that they may be putative CSLC with potential stemness. In E-cancer cells the different sized CD44+ cells were surrounded by brownish granules marker in diffuse pattern. The smaller CD44+ cells together with the CD133+ cells could be also located at the basal layer of stratified squamous epithelium, while the larger brownish CD44+ (hi) cells were mainly located in the prickle cell layer of the stratified squamous epithelium in ESCC, suggesting that they may be putative cancer progenitor cells with limited potential stemness.

Both CD133 and CD44 expressed by CSC or slightly by SC are transmembrane glycoproteins in component. The underlying biological significance of CD133 has not yet entirely elucidated, despite of some reports concerning CD133 which could participate in metastasis (Bao, et al., 2008, Pirozzi et al., 2013). Besides, increased CD133 expression level is correlated with poor prognosis in the patients with neuroblastoma or hepatocellular carcinoma (Tong et al.,2008; Song et al., 2008). CD44 glycoprotein was found not only located at the surface, but also revealed in intercellular/extracellular adhesion matrix in multifocal and diffuse pattern (Knudson, 2003). The cell surface CD44, as the hyaluronan receptor as well as the E-selectin ligand, interacts with the matrix CD44 or the CD44 variant isoforms, such as CD44v6/CD44v3, are capable of facilitating cancer growth and metastasis, and higher CD44 expression is also correlated with poor prognosis in cancer cases (Thomas et al 2008; Kobel et al, 2004). Combined CD133/ CD44 expressions is a prognostic indicator of disease-free survival in patients with colorectal cancer (Galizia et al, 2012).

NF-κB is activated by responsing to various stimuli, such as oxidant stress, immune response and carcinogenesis (Wertz and Dixit, 2010). The quercetin flavonoids are capable to act as anti-inflammatory agents via modulation of pro-inflammatory gene expression and signal transduction pathways (Tuñón,et al.,2009). Activated NF-κBp65 (RelA) and the aberrant HDAC activity play the pivotal role of tumorigenesis (Sun et al., 2012; Seidel et al., 2012). Additionally there is link between RelA/p65 and class I HDACs in nuclear translocation as well as RelA/p65 DNA binding activity (Lehmann, et al., 2009). The apoptosis is induced through inactivation of nuclear factor–kappaB and activation of caspase pathway after anti-cancer treatment (Park, et al., 2011). HDAC inhibitors are promising anti-tumor agents as they may affect the cell cycle, inhibit proliferation, stimulate differentiation and induce apoptotic cell death (Steliou,et al., 2012). In present experiment the down-regulated HDAC1 with nuclear translocation inhibited RelA/p65 activity, the down-regulated HDAC1, Rel A and Cyclin D1 and up-regulated Caspase-3 were induced by nLQ, acting as the HDAC inhibitor (HDI). The HDI, such as nLQ, can serve as a promising approach to suppress NF-κB activity which may lead to induce apoptosis through HDAC-NF-κB cascade signaling.

Epithelial-mesenchymal transition (EMT) is implicated in embryonic development and tumor metastasis (Kokkinos, et al., 2010; Wang et al., 2013). In this experiment the E-cadherin expression was up-regulated by nLQ, implicating that the EMT could be reversed by nLQ at certain extent. It is suggested that the reversal EMT induced by nLQ may inhibit cancer cell metastatic stemness potency via wnt/β-catenin pathway (Cai, et al., 2013). Almanaa TN et al indicate that the anti-stem like cell effects can be induced by phytochemical agent, curcumin, in human esophageal cancer cells (Almanaa et al., 2012), the apoptotic effect via HDAC-NF-κB cascade signaling induced by the phytochemical agent, quercetin, was studied in this experiment. We found that the apoptotic cells induced by nLQ varied in sizes, no stem cell marker was demonstrated. Then, we further studied the apoptosis induced by liposomal quercetin with cytomembrane-philia character combined with CD133 antiserum, which may contribute to endocytosis by E-cancer cells and resulted in about 6-7 % apoptotic rates promoted. The apoptotic E-cancer cells, including large and small cells in different sizes showed CD133+ marker, albeit the apoptotic signals in cells were not as clear as nLQ induced.

So far, the hypothesis that CSC derives from accumulated mutation of stem cells/progenitors with microenvironment has received strong support (Dreeson and Brivanlou, 2007), there is similarity between CSC and SC in self-renewal, multipotential and marker expression albeit with different expression levels (Gil et al., 2008;,Bu and Cao, 2012). Studies of CSC focus on exploring novel target for therapeutic/preventive intervention. Either the specific miRNA (Guo JX et al., 2012) or the labeled CSC marker (Jin, et al., 2012) can be applied to anti-CSC research as novel therapeutic strategy. Since the CD133 marker was mainly located at the cytomembrane in our experiment, the E-cancer cells apoptosis was induced with the cytomembrane-philia liposomal Q combined with CD133 antiserum to enhance apoptosis, including small CD133+ apoptotic cells. The therapeutic/preventive intervention is worth to be further investigated.

Acknowledgements

The authors thank Dr. Chenyang Chang for her valuable input, Dr. Junliang Zhao for his suggestion and Dr. Yan Feng for her careful revision.s

References

Almanaa TN, Geusz ME, Jamasbi RJ, et al (2012). Effects of curcurmin on stem-like cells in human esophageal squamous carcinoma cell lines. *BMC Complement Altern Med*, **12**, 195.

Aomatsu N, Yashiro M, Kashiwagi S, et al (2012). CD133 is a useful surrogate marker for predicting chemosensitivity to neoadjuvant chemotherapy in breast cancer. *PLoS One*, **7**, 45865.

Bao S, Wu Q, Li Z, et al (2008). Targeting cancer stem cells through L1CAM suppresses glioma growth. *Cancer Res*, **68**, 6043-48.

Bertrand J, Begaud-Grimaud G, Bessette B, et al (2009). Cancer stem cells from human glioma cell line are resistant to Fas-induced apoptosis. *Int J Oncol*, **34**, 717-27.

Bu Y, Cao D (2012). The origin of cancer stem cells. *Front Biosci*, **4**, 819-30.

Cai J, Guan H, Fang L, et al (2013). MicroRNA-374a activates Wnt/β-catenin signaling to promote breast cancer metastasis. *J Clin Invest*, **123**, 566-79.

Carcia Bueno JM, Ocaiia A, Gastro-Garcia P, et al (2008). An update on the biology of cancer stem cells in breat cancer. *Clin Transl Oncol*, **10**, 786-93.

Cetin I, Topcul M (2012). Cancer stem cells in oncology. *J BUON*, **17**, 644-8.

Charpentier MS, Whipple RA, Vitolo MI, et al (2014). Curcumin targets breast cancer stem-like cells with microtentacles that persist in mammospheres and promote reattachment. *Cancer Res*, **74**, 1250-60.

Chen YC, Hsu HS, Chen YW, et al (2008). Oct-4 expression maintained caner stem-like properties in lung cancer-derived CD133-positive cells. *PLoS ONE*, **3**, 2637.

Chu P, Clanton DJ, Snipas TS, et al (2009). Characterization of a subpopulation of colon cancer cells with stem cell-like properties. *Int J Cancer*, **124**, 1312-21.

Dreeson O, Brivanlou AH (2007). Signaling pathways in cancer and embryonic stem cells. *Stem Cell Rev*, **3**, 7-17.

Galizia G, Cemei M, Del Vecchio L, et al (2012). Combined CD133/CD44 expression as a prognostic indicator of disease-free survival in patients with colorectal cancer. *Arch Surg*, **147**, 18-24.

Gil J, Stembalska A, Pesz KA, Sasiadek MM (2008). Cancer stem cells: the theory and perspectives in cancer therapy. *J Appl Genet*, **49**, 193-99.

Gong CC, Zheng NG, Wu JL, et al (2009). Mechanism of quercetin anti-oxidative effect on NIH-3T3 cells *in vitro* and on rats *in vivo*. *Basic Clin Med*, **29**, 52-8.

Guo JX, Tao QS, Lou PR, et al (2012). miR-181b as a potential molecular target for anticancer therapy of gastric neoplasms. *Asian Pac J Cancer Prev*, **13**, 2263-7.

Hori Y (2013). Promini-1 (CD133) reveals new faces of pancreatic progenitor cells and cancer stem cells: current knowledge and therapeutic perspectives. *Adv Exp Med Biol*, **777**, 185-96.

Hu L, Cao D, Li Y, et al (2012). resveratrol sensitized leukemia stem cell-like KG-1a cells to cytokine-induced killer cells-mediated cytolysis through NKG2D ligands and TRAIL receptors. *Cancer Biol Ther*, **13**, 516-26.

Jin ZH, Sogawa C, Furukawa TY et al (2012). Basic studies on radioimmunotargeting of CD133-positive HCT116 cancer stem cells. *Mol Imaging*, **11**, 445-50.

Kobel M, Weichert W, Cruwell K, et al (2004). Epithelial hyaluronic acid and CD44v6 are mutually involved in invasion of colorectal adennocarcinomas and linked to patient prognosis. *Virchows Arch*, **445**, 456-64.

Kokkinos MI, Murthi P, Wafai R, et al (2010). Cadherins in the human placenta-epithelial-mesenchymal transition (EMT) and placental development. *Placenta*, **31**, 747-55.

Knudson CB (2003). Hyaluronan and CD44: strategic players for cell-matrix interactions during chondrogenesis and matrix assembly. *Birth Defects Res Part C: Embryo Today*, **69**, 174-96.

Lehmann A, Denkert C, Budczies J, et al (2009). High class I HDAC activity and expression are associated with RelA/p65 activation in pancreatic cancer *in vitro* and *in vivo*. *BMC Cancer*, **9**, 395.

Park MH, Choi MS, Kwak DH, et al (2011). Anti-cancer effect of bee venom in prostate cancer cells through activation of caspase pathway via inactivation of NF-ϰB. *Prostate*, **71**, 801-12.

Pellacani D, Oldridge EE, Collins AT, Maitland NJ (2013). Promini-1 (CD133) expression in the prostate and prostate cancer: a marker for quiescent stem cells. *Adv Exp Med Biol*, **777**, 167-84.

Pincelli C, Marconi A (2010). Keratinocyte stem cells: friends and foes. *J Cell Physiol*, **225**, 310-5.

Pincelli C, Marconi D, Milsom C, Magnus N, et al (2010). Role of the tissue factor pathway in the biology of tumor initiating cells. *Thromb Res*, **125**, 44-50.

Pirozzi G, Tirino V, Camerlingo R, et al (2013). Prognostic value of cancer stem cells, epithelial-mesenchymal transition and circulating tumor cells in lung cancer. *Oncol Rep*, **29**, 1763-8.

Puglisi MA, Sgambato A, Saulnier N F, et al (2009). Isolation and characterization of $CD133^+$ cell population within human primary and metastatic colon cancer. *Eur Rev Med Pharmacol Sci*, **1**, 55-62.

Seidel C, Schnekenburger M, Dicato M, Diederich M (2012). Histone deacetylase modulators provided by mother nature. *Genes Nutr*, **7**, 357-67.

Simon RA, di Sant'Agnese PA, Huang LS, et al (2009). CD44 expression is a feature of prostatic small cell carcinoma and distinguishes it from its mimickers. *Hum Pathol*, **40**, 252-8.

Song W, Li H, Tao K, et al (2008). Expression and clinical significance of the stem cell marker CD133 in hepatocellular carcinoma. *Int J Clin Pract*, **62**, 1212-8.

Sun WJ, Zhou X, Zheng JH, et al (2012). Histone acetyltransferases and deacetylases: molecular and clinical implications to gastro- intestinal carcinogenesis. *Acta Biochim Biophys Sin*, **44**, 80-91.

Steliou K, Boosalis MS, Perrine SP, et al (2012). Butyrate histone deacetylase inhibitors. *Biores Open Access*, **1**, 192-8.

Tabu K, Bizen N, Taga T, Tanaka S (2013). Gene regulation of Prominin-1(CD133) in normal and cancerous tissues. *Adv Exp Med Biol*, **777**, 73-85.

Thomas SN, Zhu F, Schnaar PL, et al (2008). Carcinoembryonic antigen and CD44 variant isoforms cooperate to mediate colon carcinoma cell adhesion to E- and L-selectin in shear flow. *J Biol Chem*, **283**, 15647-55.

Tong QS, Zheng LD, Tang ST, et al (2008). Expression and clinical significance of stem cell marker CD133 in human neuroblastoma. *World J Pediatr*, **4**, 58-62.

Tuñón MJ, García-Mediavilla MV, Sanchez-Campos S, González-Gallego J (2009). Potential of flavonoids as anti-inflammatory agents: modulation of pro- inflammatory gene expression and signal transduction pathways. *Curr Drug Metab*, **10**, 256-71.

Wang F, Qi Y, Li X, et al (2013). HDAC inhibitor trichostatin A suppresses esophageal squamous cell carcinoma metastasis through HADC2 reduced MMP-2/9. *Clin Invest Med*, **36**, 87-94.

Wang K, Xu J, Zhang J, Huang J, et al (2012). Prognostic role of CD133 expression in colorectal cancer: a meta-analysis. *BMC Cancer*, **12**, 573.

Wertz IE, Dixit VM (2010). Signaling to NF-kappaB: regulation by ubiquitination. *Cold Spring Harb Perspect Biol*, **2**, 3350.

Zhang Qinxian, Zheng Naigang, Zhang Ying, et al (2007). Redox-evolution of Eca-109 cells by 8-Br-cAMP and quercetin and correlation with p16ss DNA binding nuclear matrix protein. *Life Sci J*, **4**, 1-7.

Zheng Naigang, Wang Li, Wu Jinglan, et al (2008). Rapid enrichment of stem cell population by filter screening and biomarker-immunoassays from human epidermis. *Life Sci J*, **5**, 33-7.